JOURNAL OF VIROLOGY, Nov. 2011, p. 12001–12012 Vol. 85, No. 22
0022-538X/11/$12.00 doi:10.1128/JVI.05567-11
Copyright © 2011, American Society for Microbiology. All Rights Reserved.

Conformation-Selective Methylation of Geminivirus DNA[▽]

T. Paprotka,† K. Deuschle, V. Metzler, and H. Jeske*

Biologisches Institut, Abteilung für Molekularbiologie und Virologie der Pflanzen, Universität Stuttgart, Pfaffenwaldring 57, D-70550 Stuttgart, Germany

Received 30 June 2011/Accepted 29 July 2011

Geminiviruses with small circular single-stranded DNA genomes replicate in plant cell nuclei by using various double-stranded DNA (dsDNA) intermediates: distinct open circular and covalently closed circular as well as heterogeneous linear DNA. Their DNA may be methylated partially at cytosine residues, as detected previously by bisulfite sequencing and subsequent PCR. In order to determine the methylation patterns of the circular molecules, the DNAs of tomato yellow leaf curl Sardinia virus (TYLCSV) and Abutilon mosaic virus were investigated utilizing bisulfite treatment followed by rolling circle amplification. Shotgun sequencing of the products yielded a randomly distributed 50% rate of C maintenance after the bisulfite reaction for both viruses. However, controls with unmethylated single-stranded bacteriophage DNA resulted in the same level of C maintenance. Only one short DNA stretch within the C2/C3 promoter of TYLCSV showed hyperprotection of C, with the protection rate exceeding the threshold of the mean value plus 1 standard deviation. Similarly, the use of methylation-sensitive restriction enzymes suggested that geminiviruses escape silencing by methylation very efficiently, by either a rolling circle or recombination-dependent replication mode. In contrast, attempts to detect methylated bases positively by using methylcytosine-specific antibodies detected methylated DNA only in heterogeneous linear dsDNA, and methylation-dependent restriction enzymes revealed that the viral heterogeneous linear dsDNA was methylated preferentially.

Methylation of DNA is commonly investigated using methylation-sensitive restriction enzymes and bisulfite sequencing, which converts unmethylated cytosines into uracil. The products are usually amplified by PCR and sequenced after bacterial cloning (14, 23). The critical steps in various protocols are the complete conversion of unmethylated cytosines to uracil (26, 78) and the design of appropriate primers for the converted DNA (reviewed in references 58 and 85). Several bioinformatic tools have been developed to analyze the results (9, 46–48, 66, 71), including recent improvements for the analysis of plant DNA cytosine methylation (27, 35).

Eukaryotes methylate cytosine at C^5 by methyltransferases, which differ between plants, fungi, and mammals (reviewed in reference 25). In mammals, symmetric CpG sites are usually preferred, whereas nearly every cytosine residue in plant DNA can be methylated (reviewed in reference 5). As a result, only 2 to 8% of mammalian DNA is methylated, compared to up to 50% of DNA in higher plants (reviewed in reference 84). The methylation status is highly dynamic. In plants, demethylation is mediated by DNA glycosylases and strand cleavage (84), a mechanism which would inactivate single-stranded DNA (ssDNA). In addition to C-methylation, N^6-adenine methylation is well known for bacteria but rarely described for plants (19, 74).

The circular ssDNA-containing geminiviruses (reviewed in reference 37) are important plant pathogens causing severe damage in crop plants all over the world (49). Their DNA is packed into icosahedral twin particles (8, 83). Four geminivirus genera have been described, differing in genome organization, host range, and insect vector (67). After insect vectors have inoculated the plant, viral particles are disassembled (42) and the ssDNA is copied by complementary strand replication (CSR) to double-stranded covalently closed circular DNA (cccDNA) (31), which is packaged into nucleosomes to form minichromosomes (1, 55, 56). Further progeny DNA is replicated by rolling circle replication (RCR) as well as by recombination-dependent replication (RDR) (reviewed in reference 38), generating large amounts of heterogeneous linear dsDNA (hdsDNA).

Both geminivirus circular and linear DNAs as well as ssDNA and dsDNA may serve as templates for PCR during bisulfite sequencing of total nucleic acids, preventing the assignment of methylated nucleotides to a specific DNA conformation. Cloning, diagnosis, infection, and direct sequencing of viruses with small circular DNA genomes have been improved considerably by rolling circle amplification (RCA) with bacteriophage Phi29 polymerase (see references 29, 36, 39, 52–54, and 82 and references therein). In combination with random hexamer primers, circular DNA can be amplified preferentially from plant samples without any prior knowledge of the sequence. Therefore, it was intriguing to test this technique for the identification of C modifications by restriction analysis and bisulfite sequencing.

Geminiviruses induce small interfering RNAs (siRNAs) (2, 7, 62, 73), which may lead to posttranscriptional (PTGS) as well as transcriptional (TGS) gene silencing (4, 65). This interplay of PTGS and TGS has been understood as part of the plant defense pathways (reviewed in references 16, 64, 75, and 76). Correspondingly, geminiviruses have developed potent

* Corresponding author. Mailing address: Biologisches Institut, Abteilung für Molekularbiologie und Virologie der Pflanzen, Universität Stuttgart, Pfaffenwaldring 57, D-70550 Stuttgart, Germany. Phone: 49-711-685-65070. Fax: 49-711-685-65096. E-mail: holger.jeske@bio.uni-stuttgart.de.

† Present address: Viral Mutation Section, HIV Drug Resistance Program, National Cancer Institute at Frederick, Frederick, MD 21702.

▽ Published ahead of print on 10 August 2011.

suppressors of gene silencing (reviewed in references 6 and 61). Promoting PTGS and TGS in host plants to establish novel resistance strategies against viruses is a promising but also challenging strategy (reviewed in reference 72). Moreover, both silencing routes may be used to knock down host genes with the help of geminivirus vectors (virus-induced gene silencing [VIGS]) (12, 13, 20, 43, 45, 51). In this context, the analysis of the methylation status of geminivirus episomal or integrated DNA has revealed important insights (4, 11, 28, 60, 62, 65).

Several lines of evidence for the relevance of C-methylation during geminivirus infection have been described. (i) Viral replication in protoplasts was inhibited if the transfected DNA was methylated before inoculation (10, 18). (ii) *Arabidopsis* plants which were defective in the genes for key enzymes of the transcriptional gene silencing pathway, including cytosine methyltransferases, methyl cycle enzymes, and Dicer-like proteins, developed more severe symptoms than wild-type (wt) plants did (60). (iii) Transgenes which were expressed under the control of geminivirus promoters were silenced, and their cytosines methylated, if the plants were superinfected with the corresponding virus, and in complement, an increased level of C-methylation was observed for the replicated DNA (4, 65). (iv) Recovery of plants was accompanied by elevated C-methylation of geminivirus DNA (28, 60, 62). (v) Geminivirus suppressors of silencing changed the global methylation profile of plants (11).

All investigations with respect to sequence-specific DNA methylation have been based on the PCR technique and were thus not able to discriminate between the multitude of geminivirus DNA forms described (3, 17, 40, 41, 59). In particular, we were interested in determining whether there are differences in methylation between heterogeneous linear dsDNA and the circular dsDNA conformers. To this end, various methods based on RCA were tested in order to determine the contribution of C-methylation to the circular population of geminivirus DNAs. The results allowed, for the first time, a broad statistical approach to validate the relevance of C-methylation for complete genome components. Two distinct viruses in the genus *Begomovirus* were chosen as examples: an Old World and monopartite representative, tomato yellow leaf curl Sardinia virus (TYLCSV) (50), and a New World bipartite representative, Abutilon mosaic virus (AbMV) (22). Both viruses were investigated during the course of systemic infection in the experimental model plant *Nicotiana benthamiana* (79).

MATERIALS AND METHODS

Microorganisms and plants. Agroinfectious clones of TYLCSV (L27708) (50) and AbMV (X15983 and X15984) (22) were inoculated into the experimental host *Nicotiana benthamiana* Domin and grown in a greenhouse with supplementary lighting or in a climate chamber as described previously (81), under containment according to gene technology license S2. The *Escherichia coli* bacteria and phages used have been described previously (34). In addition, leaves of naturally occurring AbMV-infected ornamental *Abutilon* plants (80) were used.

Total nucleic acid extraction. Total nucleic acids were extracted from 0.1 to 0.2 g systemically infected upper leaves that were harvested between 9 and 10 a.m. as described previously (29, 40). DNA amounts were quantified by the aid of 4′,6-diamidino-2-phenylindole (DAPI) (69) fluorescence compared to a lambda DNA standard with defined concentrations.

Methylation-sensitive restriction enzyme analysis. Total nucleic acids were digested by either of the isoschizomer pairs MspI-HpaII and Sau3A-MboI, using 300 ng total DNA per reaction mix, supplemented with 300 ng of λ DNA to control the completeness of the digestion. Restriction enzymes (10 U of each) and RNase A (0.5 mg/ml) were added and incubated overnight at 37°C. Samples were separated in 1.4% agarose gels (3 h, 120 V). As restriction fragment length polymorphism (RFLP) standards, 1-μl samples of 1:50-diluted RCA products (TempliPhi kit; GE Healthcare, Munich, Germany) from total nucleic acids of AbMV- or TYLCSV-infected plants were digested in parallel. Southern blots were hybridized as described previously (81), using digoxigenin (DIG)-labeled DNA probes (Roche, Mannheim, Germany) from full-length viral fragments.

Methylation-dependent restriction enzyme analysis. Total nucleic acids were digested by McrBC (NEB, Frankfurt, Germany), using 200 ng total DNA per reaction mixture, supplemented with 100 μg/ml bovine serum albumin (BSA), 1 mM GTP, and 15 U of the restriction enzyme, at 37°C overnight. Undigested samples were treated in the same way but without adding the enzyme. The samples (60 ng of DNA for each) were separated in 1.4% agarose gels containing 20 μg/ml or 50 μg/ml chloroquine (19 h, 40 V). As a loading control and to ensure the completeness of digestion, samples were separated in parallel in 1.4% agarose gels, which then were stained with ethidium bromide. Southern blots were hybridized as described above (81), using viral probes lacking the intergenic region.

Two-dimensional (2D) agarose gel electrophoresis (1st dimension with 0.3% SDS and 2nd dimension with 20 μg/ml chloroquine) was performed with 100 ng total DNA per sample, as described previously (40).

Separation of dsDNA and ssDNA. Single-stranded and double-stranded DNA intermediates were separated on benzoylated naphthoylated DEAE (BND) cellulose (Sigma) as described previously (59). Total DNA (1.5 μg) was loaded onto the matrices and eluted with increasing salt concentrations (0.4 to 1.25 M NaCl) according to the manufacturer's recommendations. Nucleic acids were collected by ethanol precipitation (63) and dissolved in 20 μl sterile water.

Sample preparation for bisulfite conversion. The wash fraction from BND chromatography, which was enriched in dsDNA, was used for bisulfite conversion. Based on previous reports (23, 26, 78), RNA- and protein-free samples were used to promote complete conversion of unmethylated cytosines. Samples (20 μl) were treated with 1 mg/ml RNase A for 2 h 30 min, followed by 1 mg/ml proteinase K overnight. Proteins were removed by two phenol-chloroform-isoamyl alcohol (25:24:1) extractions, one chloroform extraction, and ethanol precipitation (63). DNA was dissolved in 20 μl nuclease-free water and converted using an EpiTect bisulfite conversion kit (Qiagen, Hilden, Germany) according to the manufacturer's protocol. The conversion rate of cytosines was validated by two control experiments. The 5S rRNA gene was partially sequenced using the primer pair 5′-TAAGAAAATCTAGAGTGTAAGGAATGTTGGATGCGATTATAT-3′ and 5′-TTCATTAATACAAGCTTTACCAAAAAAAAAAATACAACACGAAA-3′, as previously described for the bisulfite-converted top strand (4, 24). The bacterial plasmid pBluescript II SK(−) (Stratagene, Amsterdam, Netherlands), with a size similar to that of geminivirus DNA (2,961 bp), was transreplicated with the help of phage R408 to obtain artificial standard phage progeny lacking methylation as described previously (34). Phage corresponding to 10, 50, 100, or 1,000 ng of ssDNA were mixed with leaf samples from uninfected plants, and DNA extraction was performed as described for virus-infected plant tissue.

One volume of converted DNA was added to 10 volumes of an RCA reaction mixture prepared by use of a TempliPhi kit (GE Healthcare, Munich, Germany), and in order to preserve the labile converted DNA, the reaction was performed at 4°C for 72 h, a critical prerequisite for obtaining final products.

Random cloning and sequencing of bisulfite-treated DNA. RCA products (15 μl of each) from bisulfite-treated DNA were digested with 60 U DraI (New England BioLabs, Frankfurt am Main, Germany) in a volume of 50 μl, ethanol precipitated, and ligated (63) into the EcoRV site of pBluescript SK II(+) (50 ng) in a volume of 10 μl. The product was transformed into *E. coli* DH5α and plated on LB agar containing ampicillin, X-Gal (5-bromo-4-chloro-3-indolyl-β-D-galactopyranoside), and IPTG (isopropyl-β-D-thiogalactopyranoside). Positive clones were selected by blue-white screening followed by colony RCA. The presence of inserts was checked by digestion with BamHI and ClaI. Sequencing was performed at Macrogene (South Korea), using universal M13 forward primers. Sequences were analyzed using NCBI BLASTN and sorted. Viral fragments were assembled with the corresponding genomes by using the CAP contig assembly program included in BioEdit 7 software (30), and the numbers of converted nucleotides were determined with the help of Microsoft Excel.

Identification of methylated DNA in Southern blots by comparing hybridization and immunolabeling. 2D gel electrophoresis (1st dimension with SDS and 2nd dimension with chloroquine) was performed with 1 μg total DNA per sample as described previously (40). One of two parallel gels was processed as described previously (40), and the DNA in the second gel was blotted under neutral conditions (20× SSC [3 M NaCl plus 0.3 M sodium citrate, pH 7.0]) onto a nitrocellulose membrane (Protran; Whatman, Dassel, Germany) and UV

cross-linked (2 min, 700 μJ/cm^2, 254-nm UV) (Amersham). The second membrane was blocked for 1 h in 1% blocking reagent (BR; Roche, Mannheim, Germany) in PI (0.1 M maleic acid, 150 mM NaCl, pH 7.5), incubated for 1 h with an N^5-methylcytosine (m5C)-specific mouse antibody (33D3; Aviva, San Diego, CA) diluted 1:5,000 in 1% BR in PI, washed three times for 15 min with PI supplied with 0.03% Tween 20 (Roth, Karlsruhe, Germany), and incubated with an anti-mouse–horseradish peroxidase (HRP) antibody conjugate (1:10,000 in 1% BR in PI) (Rockland, Gilbertsville, PA) for 45 min. After three 15-min washings in PI with 0.03% Tween 20, the membrane was incubated for 15 min in phosphate-buffered saline (PBS; 0.137 M NaCl, 6.5 mM Na_2HPO_4, 2 mM NaH_2PO_4, pH 7.4) and developed using a chemiluminescence reaction (ECL Femto; Pierce, Rockford, IL) according to the manufacturer's protocol.

RESULTS

Nucleotide methylation at restriction enzyme recognition sites. Nucleotide methylation can be inferred by the use of isoschizomer pairs of restriction endonucleases which are sensitive or insensitive to methylated nucleotides (reviewed in references 68, 85, and 86). A previous study found no cytosine methylation with isoschizomer pairs for tomato golden mosaic geminivirus but a decrease of infectivity for *in vitro*-methylated DNA (10). To test the methylation at specific sites for TYLCSV and AbMV, total nucleic acid extracts were harvested during the time course of systemic infections, at 14, 21, and 49 days postinfection (dpi), digested with each of the isoschizomer pairs MspI-HpaII and Sau3AI-MboI, and analyzed by blot hybridization (Fig. 1). RCA products from infected plants, used in parallel, served as controls for completely unmethylated DNA (Fig. 1, lanes C). To test the completeness of the enzyme reaction under the chosen conditions, equal amounts of bacteriophage λ DNA were mixed with the target DNA and analyzed in ethidium bromide-stained gels (Fig. 1a and c).

MspI and HpaII share the recognition sequence CCGG. Whereas HpaII is blocked if any one of the cytosines is methylated, MspI can cut if the internal (but not external) C is methylated (44). The Southern blots in Fig. 1b and d show that for both geminiviruses, the majority of hybridization signals for the cut viral dsDNAs comigrated with the RCA fragments, indicating that the restriction of most viral dsDNA molecules was not affected by methylation. Only minor bands (Fig. 1b and d, black asterisks) deviated from this general conclusion and might indicate base modifications. However, none of these bands differed between both isoschizomer treatments for all time points of harvest. Such a result may have been caused by general methylation of both or the external cytosines, or the bands may represent mutated molecules within the viral quasispecies population, without any contribution of base modifications. They also may have originated from DNA molecules that did not replicate completely during complementary strand synthesis *in vivo* or from incomplete digestion.

Sau3AI and MboI share the recognition sequence GATC. According to the supplier's information (New England BioLabs), both enzymes are equally impaired by cytosine methylation at the C in the recognition sequence and are differentially active only for N^6-adenine. The plant DNA was cut differentially by the two enzymes (Fig. 1a and c), suggesting that adenines were modified in these plants (74).

The interpretation of the restriction patterns on the corresponding Southern blots (Fig. 1b and d) was impaired partially by the appearance of viral ssDNA in TYLCSV fragment detection, in particular during late infection. ssDNA generally appeared as more diffuse bands (Fig. 1b, ss band) and interfered especially when defective DNAs had accumulated (Fig. 1b, lanes for 49 dpi). Compared to the RCA product controls, only two minor differential bands (Fig. 1b, white asterisks) appeared after Sau3AI digestion but not after MboI digestion. This result is unexpected and difficult to explain, since Sau3AI should be the more effective isoschizomer in this comparison.

These initial experiments indicated that methylated viral DNA, if present, was a minor fraction of the total viral dsDNA during the analyzed time course of infection in emerging leaves. However, we had screened only a small portion of the putatively methylated sequences. To explore this question further, we employed bisulfite sequencing, which selects positively for those sequences with m5C.

Bisulfite-treated DNA can be amplified by rolling circle amplification. The bisulfite reaction promotes deamination of C to U, which is read as T after amplification of the target sequence, whereas m5C is protected from this conversion. However, the target DNA becomes instable during the reaction, and strand breakage removes the majority of molecules from the DNA pool under investigation (78; data not shown). This effect leads in the end to an enrichment of protected or nonreacted C's in the resulting sequencing data. High-temperature treatment promotes this bias, and the longer the target sequence, the stronger is the relative selection process for nonconverted cytosines. The resulting well-known problems, in particular with quantification in combination with PCR, have been reviewed carefully (78).

We reasoned that processing the bisulfite-treated DNA at lower temperatures could reduce this problem. Therefore, PCR was replaced by RCA to amplify the target DNA after the conventional bisulfite reaction. In addition, this technique is not dependent on an elaborate choice of specific primers, thus reducing a further bias in the results. RCA selects positively for circular DNA molecules, allowing a conformation-selective view of the replication intermediates.

In initial experiments, the denaturation step (95°C for 3 min) in the standard RCA protocol dramatically decreased the amount of RCA products obtained with bisulfite-treated templates (data not shown). Because the majority of bisulfite-treated DNA is single stranded anyway (23), the denaturation step was omitted and the complete temperature regimen was lowered to 4°C. To compensate for the lower activity of the Phi29 polymerase at 4°C, the incubation time was extended to 72 h, which resulted in reasonable levels of RCA products (Fig. 2 and 3). This outcome shows for the first time that a proofreading polymerase with high fidelity is able to replicate on U-containing templates (78).

In order to monitor the efficiencies of conversion and subsequent amplification reactions, the final products were digested with two restriction enzymes which yielded complementary results in parallel: HpaII (CCGG), with only C's and G's in the recognition sequence, and DraI (TTTAAA), with only A's and T's in the recognition sequence (Fig. 2 and 3). Upon RCA/RFLP analysis, HpaII sites would survive the bisulfite treatment if their C's were methylated, and the resulting population would be detectable as remaining bands at the position of control DNA (Fig. 2 and 3). Complementary bisulfite treatment would generate seven new diagnostic DraI sites (CCCAAA, TCCAAA, TTCAAA, CTTAAA, CCTAAA,

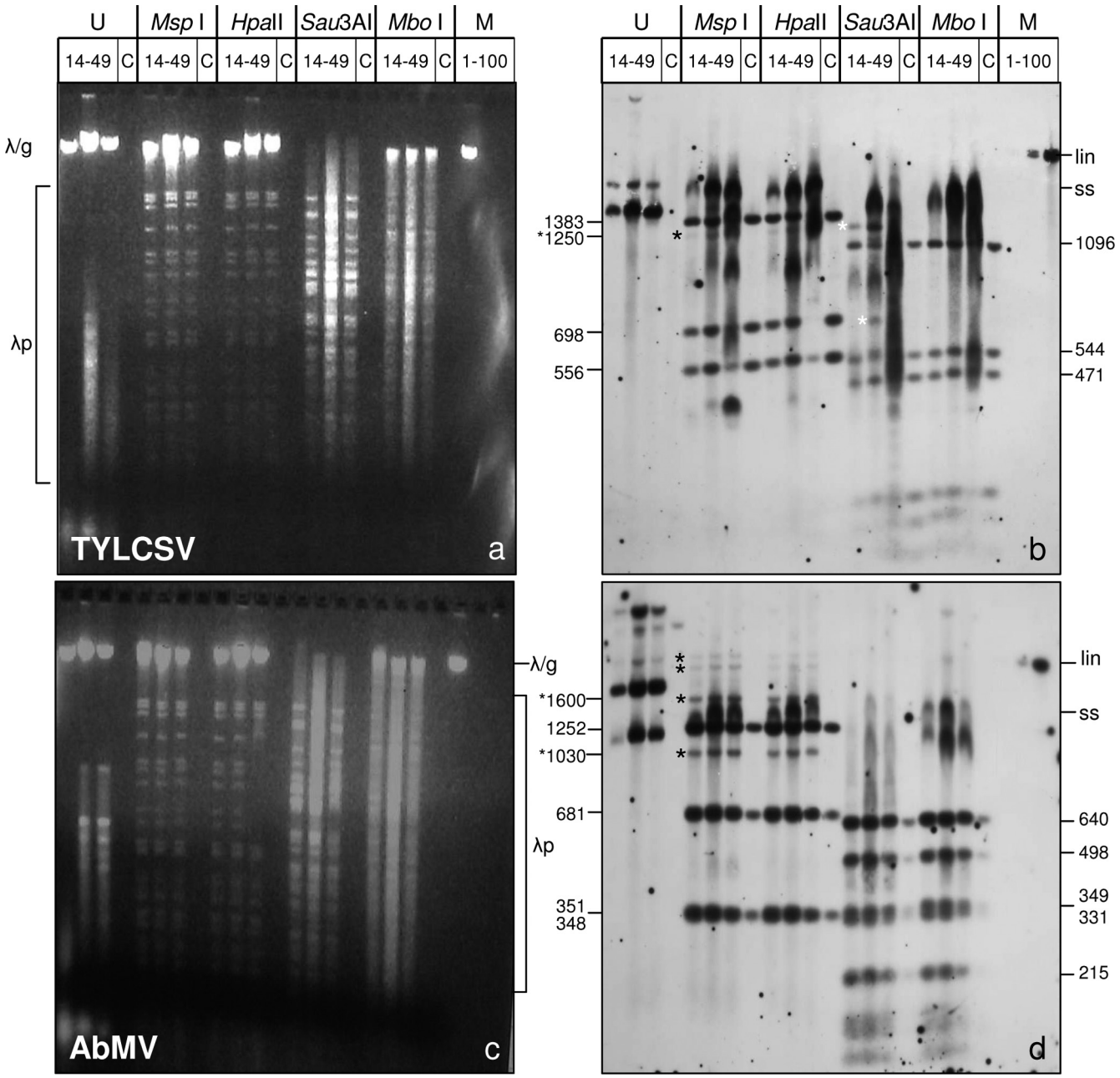

FIG. 1. Methylation-sensitive restriction enzyme digestion of viral DNA by use of isoschizomers. Total nucleic acids (300 ng DNA [each]) from *N. benthamiana* plants infected systemically with AbMV or TYLCSV and harvested at 14, 21, or 49 dpi were digested with two sets of isoschizomers: MspI (blocked by cytosine methylation of the external C) with HpaII (blocked by each of the cytosine methylations) (at CCGG) and Sau3AI (blocked by cytosine methylation but not by adenine methylation) with MboI (blocked by cytosine as well as adenine methylation) (at GATC). Untreated samples (U) with the same amounts of DNA were loaded in parallel. The samples were electrophoresed in 1.4% agarose gels (3 h, 120 V), stained with ethidium bromide (a and c), blotted onto nylon membranes, and detected with virus-specific full-length probes for TYLCSV (b) and AbMV A (d). RCA products (1 μl; diluted 1:50) from correspondingly infected plants were digested with the respective enzymes and served as size markers for completely unmethylated DNA fragments (C). Hybridization standards (M) were 1, 10, or 100 pg of linearized full-length dsDNA fragments (lin) of AbMV or TYLCSV. In order to control the completeness of digestion, 300 ng of lambda DNA was supplied to each enzyme reaction mix, forming band patterns (λp) in ethidium bromide-stained gels. Undigested λ DNA was expected to migrate to the same position as genomic plant DNA (λ/g). Geminivirus fragments which were not detected in the controls are marked by black and white asterisks. Expected fragment sizes (in base pairs) of the respective digestion products, calculated from the sequences, are shown to the left and right of the panels. Note that ssDNA tends to smear and to create more diffuse bands than those of dsDNA, as seen after Southern blot hybridization. Bands in undigested samples of ethidium bromide-stained gels refer to the usual genomic DNA and host RNA species (not indicated).

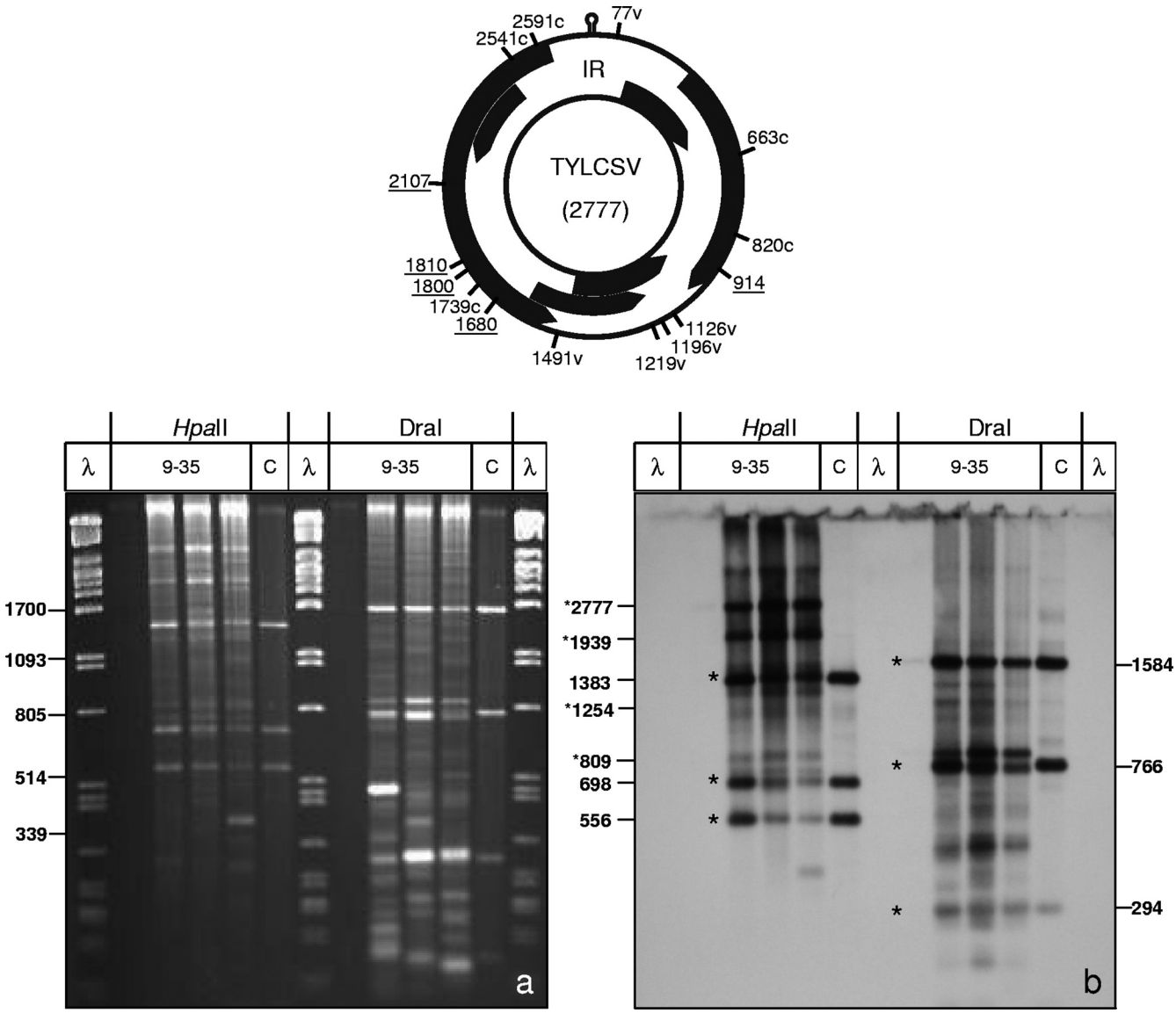

FIG. 2. RCA/RFLP analysis of bisulfite-treated DNA. The genome map of TYLCSV shows DraI sites which are present in the source DNA (underlined) or which may be created on the viral (v) or complementary (c) strand after bisulfite treatment. Total nucleic acids from systemically TYLCSV-infected *N. benthamiana* plants at 9, 14, 20, and 35 dpi were converted by bisulfite treatment and amplified by RCA. Three-microliter samples of these products were digested with HpaII or DraI, separated in 1.4% agarose gels (3 h, 120 V), and then stained with ethidium bromide (a) and Southern blotted (b). As controls (C), similarly digested RCA products (1 μl) of untreated samples were applied. The gels were blotted onto nylon membranes and detected with a full-length virus DNA probe specific for TYLCSV. The remaining fragments of unconverted molecules are marked by asterisks. No RCA product was obtained in the sample from 9 dpi.

CTCAAA, and TCTAAA) due to C-to-T exchange. Screening for such sites (genome maps in Fig. 2 and 3) revealed 7 in viral orientation and 11 in complementary orientation for TYLCSV, 1 in viral orientation for AbMV DNA A, and 2 in viral orientation and 9 in complementary orientation for AbMV DNA B. In comparison to the control DNA (Fig. 2 and 3, lanes C), remaining bands would indicate protection against the bisulfite reaction.

Systemically infected samples were analyzed at 9, 14, 20, and 35 dpi (Fig. 2 and 3, lanes 9-35). Fragment patterns changed and deviated from controls for both viruses. Prominent shifts to larger fragments than those for control DNA upon HpaII digestion (Fig. 2 and 3, asterisks) indicated that several sites were no longer recognized by this enzyme. For DraI, the appearance of smaller fragments documented the same effect. Similar results were obtained for the restriction enzymes SspI (AATATT) and RsaI (GTAC) (data not shown). Only minor variations were observed when band patterns from samples harvested at different time points after inoculation were compared. These results show that RCA/RFLP analysis is an efficient novel tool for monitoring restriction site changes after bisulfite treatment, providing the opportunity to monitor complete viral genome components without the bias of primer selection during PCR.

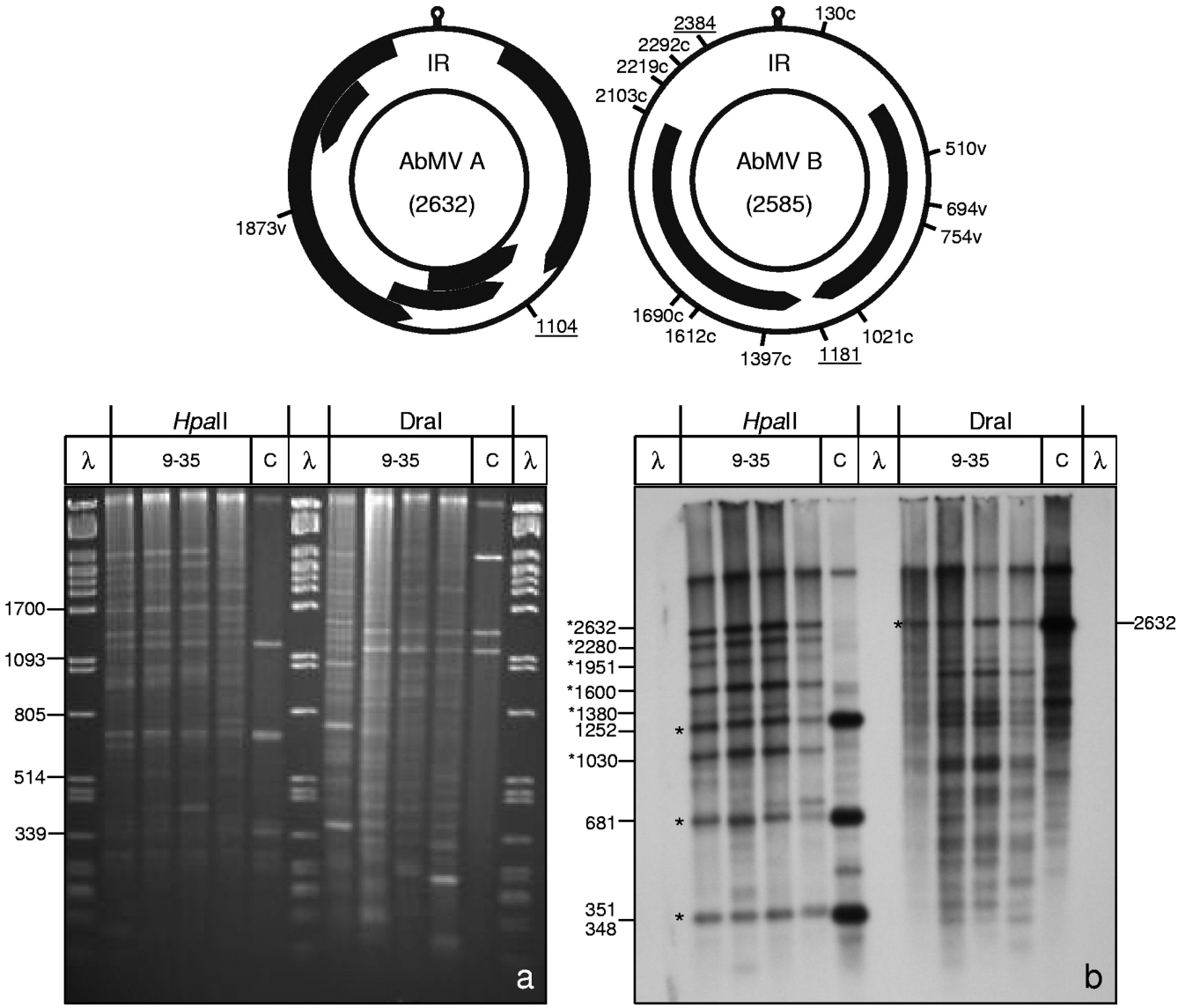

FIG. 3. Analysis of AbMV DNA as described in the legend to Fig. 2, but with detection with a full-length virus DNA probe specific for AbMV DNA A.

Random cloning of RCA products. In addition, the RCA/RFLP procedure was ideal for identifying exact sequence positions of converted cytosines. The RCA products of bisulfite-treated DNAs were cleaved with DraI and inserted into a plasmid's EcoRV site by blunt-end ligation, allowing random cloning of the target DNA. The sequences determined for the resulting cloned DNAs were selected for those with similarity to the viral DNA components. For TYLCSV, 60% of 25,892 sequenced nucleotides (nt) were derived from viral DNAs, and for AbMV, 68% of 17,231 sequenced nt were so derived. As expected from the few existing or potentially obtainable DraI sites in AbMV DNA A (Fig. 3, genomic map), the AbMV DNA B-derived clones were strongly overrepresented. Due to this bias, only the complete sequences of TYLCSV and the AbMV DNA B component were covered by sequencing and were analyzed in further detail. Because no significant differences in the results were obtained for samples harvested at different time points and the presence of protected C's appeared stochastically in all clones, we analyzed the information in the pooled data sets for the two viruses. Classes of 100 nt per genome segment were built, and the percentages of protected C's were averaged for each class (Fig. 4b). In addition, the distributions of the frequencies (Fig. 4c) were determined for these classes.

For TYLCSV, 51% ± 11% of 2,249 analyzed cytosines were protected, with 53% protection for CG, 50% for CNG, and 50% for CHH sites. A single short sequence (nt 1800 to 2000) revealed a considerable increase in the frequency of protected C's (Fig. 4d) (with 90% protected C's on the viral strand and 83% protected C's on the complementary strand). This sequence is located within the C1 open reading frame (ORF), in the promoter for the C2/C3 transcript. For AbMV, 53% ± 13% of 2,042 analyzed cytosines were protected, with 50% protection for CG, 52% for CNG, and 54% for CHH sites.

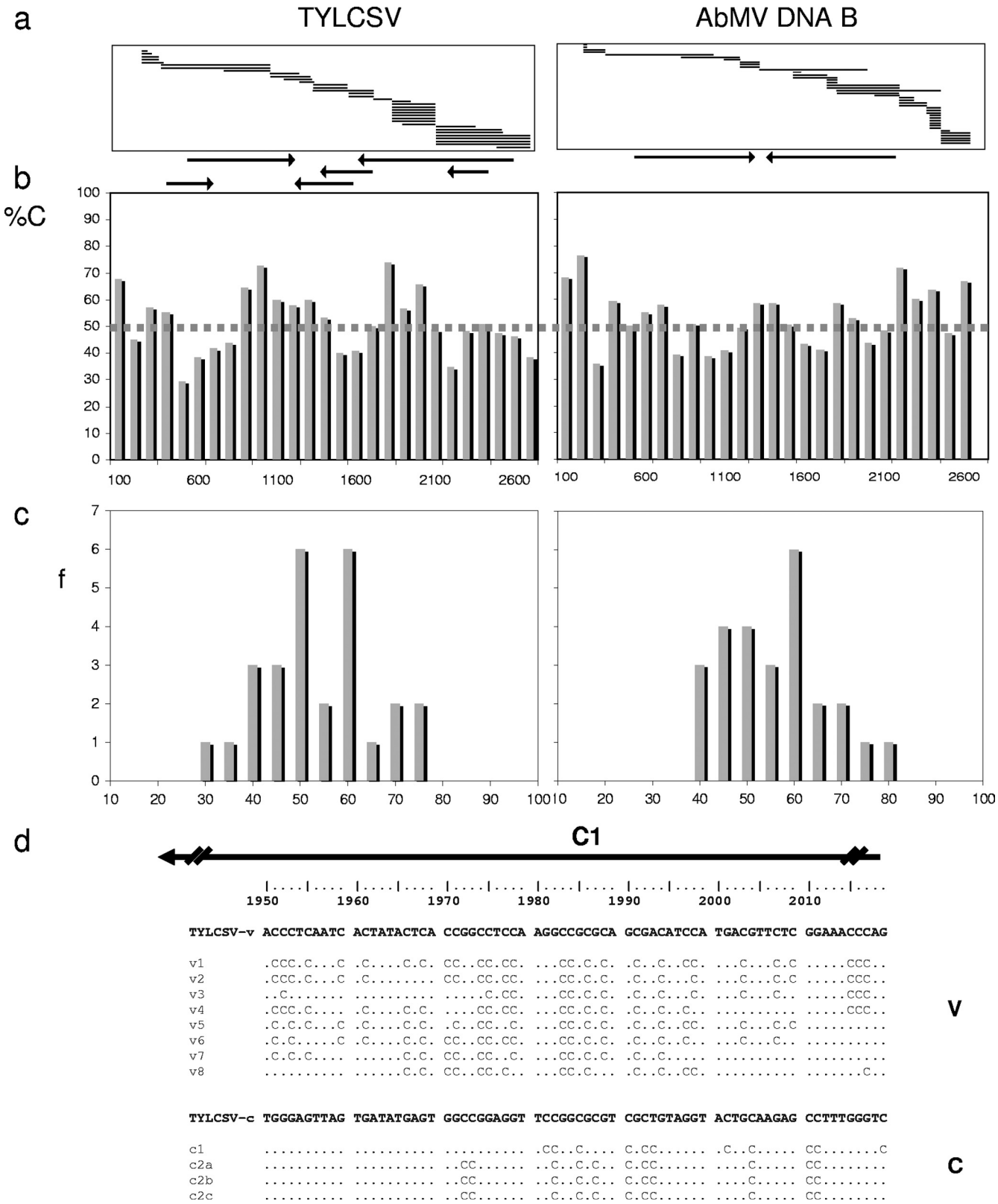

FIG. 4. Overall cytosine methylation of the TYLCSV viral strand and AbMV DNA B complementary strand. (a) Distributions of fragments obtained after sequencing of DraI-digested randomly cloned RCA products. Positions of the ORFs are marked with arrows. (b) Frequencies of protected C's in classes of 100 nt (%C) are represented by bars, and the threshold value for unmethylated phage DNA is shown as a dashed line. (c) Distribution of frequencies (f) for all class results. (d) An exceptionally protected stretch of TYLCSV is exemplified for the viral (v) and complementary (c) strands.

These results indicate a stochastic appearance of protected C's, with no significant difference between the viruses and the potential methylation sites.

To judge these results, proper controls became essential. First, the frequently used control of sequencing PCR-amplified 5S rRNA gene segments (see Materials and Methods) was applied and revealed a complete conversion of all C's (data not shown). Subsequently, a novel control was developed and led to a totally different judgment of the results obtained. Circular single-stranded DNA from pBluescript-derived artificial bacteriophages was mixed with plant samples in amounts which were similar to those of viral DNAs in systemically infected tissues and then treated in the same way as infected samples. Cloning and sequencing of the control DNAs revealed 50% protected C's among 761 C's analyzed. Thus, we determined, for the first time, a more reliable threshold for the baseline of the experiments (Fig. 4b, dotted line). Since the experimentally determined data for TYLCSV and AbMV DNA B followed mainly Gaussian distributions (Fig. 4c), only values with significant increases above the threshold may indicate true methylation as a source for the protection of C's. The C2/3 promoter region within ORF C1 of TYLCSV was the only genome portion for which the methylation rate significantly surpassed this threshold level among the circular geminivirus DNAs analyzed (Fig. 4c).

Methylation-dependent restriction analysis. In contrast to the aforementioned experimental strategies, which relied on indirect detection of methylated cytosines, the following experiments allowed their positive detection. Enzymes which cut DNA only if cytosines are methylated are excellent tools for monitoring epigenetic changes (15). After using one of them (McrBC), most of the plant DNA was digested (Fig. 5, loading controls). Viral DNAs, either digested with the enzyme or treated similarly without enzyme (Fig. 5, E+ and E− lanes), were resolved in one-dimensional chloroquine-containing agarose gels for optimal resolution of their different conformations, as shown previously (17, 56). Under these conditions, the most prominent and reproducible effects were the reduction of multimeric DNA (Fig. 5, m bands) and the appearance of more linear DNA of genomic size (Fig. 5, lin bands). Open circular (oc) and single-stranded (ss) DNAs remained stable. Supercoiled DNA (cccDNA) was reduced to a certain extent in some but not all samples, indicating a differential and dynamic change of its modification during the course of infection, more at late sampling times but stochastically by nature. Four independent replications of the time course experiments for each of the two viruses revealed no general trend for the diminishing of cccDNA after McrBC treatment. It thus remains to be determined which experimental factor enhances the putative methylation of cccDNA. As observed previously (17), ocDNA levels remained constant during the course of infection and could be used as internal controls to estimate equal loading of the sample pairs. Although the reason for the constant amount of the ocDNA portion is unknown, this observation was confirmed by four independent sets of experiments (Fig. 5 and unpublished results).

Immunolabeling of 5-methylcytosine. To further explore the conformation dependence of geminivirus DNA, AbMV DNA was separated by 2D gel electrophoresis, which enabled the discrimination of circular and linear DNAs and of ds- and

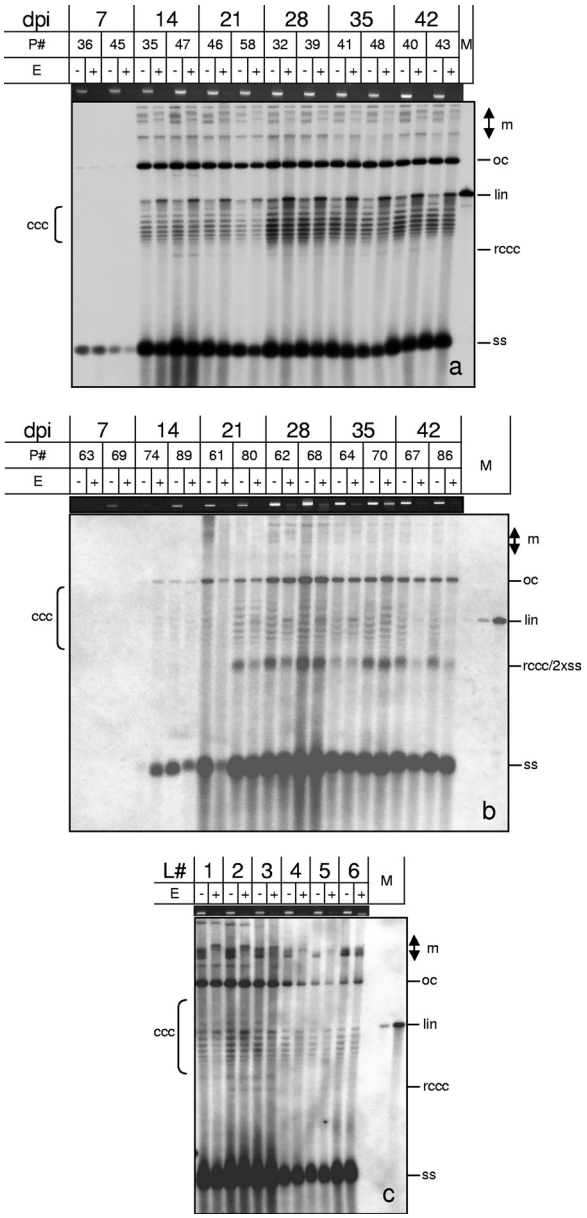

FIG. 5. Methylation-dependent restriction enzyme digestion of AbMV (a)- or TYLCSV (b)-infected *N. benthamiana* plants (P#, plant numbers) harvested at the indicated dpi. (c) In addition, individual leaves (L#, starting with the youngest leaf as L1) of ornamental *Abutilon* plants which were naturally infected with AbMV were collected. Total nucleic acids (60 ng DNA [each]) were digested with McrBC (E+) or not digested (E−), separated electrophoretically in 1.4% agarose gels containing chloroquine (50 μg/ml [a] or 20 μg/ml [b and c]), and analyzed by Southern blot hybridization against the respective probes (AbMV DNA A or TYLSCV lacking each intergenic region). Viral DNA forms are indicated as described in the legend to Fig. 1 and also as multimeric (m), open circular (oc), or relaxed covalently closed circular (rccc) DNA. As a loading control and to ensure complete digestion, equal amounts of every sample were separated in parallel in 1.4% agarose gels and stained with ethidium bromide to show the genomic plant DNA. Hybridization standards (M) were 100 pg (a) or 1, 10, or 100 pg (b and c) of linearized full-length dsDNA fragments (lin) of AbMV DNA A or TYLCSV. For each time point, two of five plants were selected randomly and used for digestion (a and b).

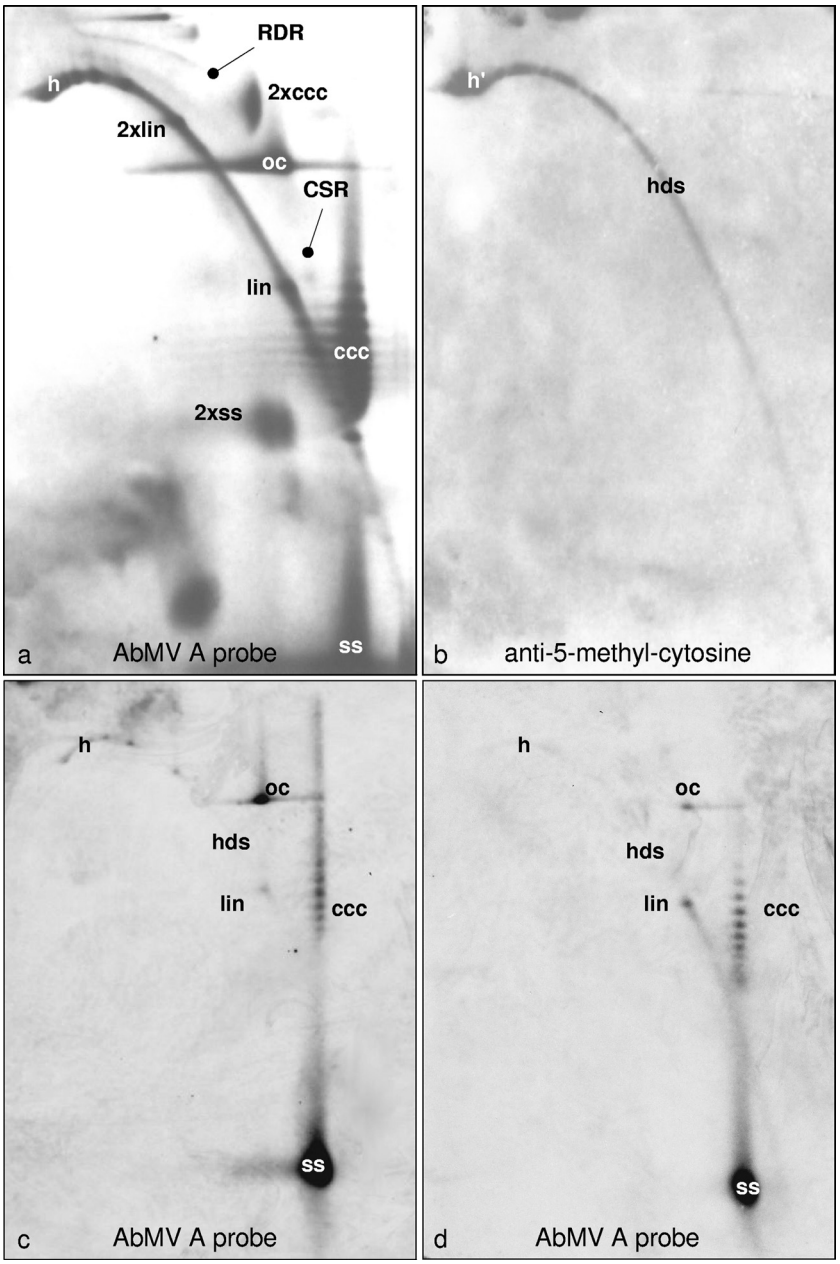

FIG. 6. Positive detection of methylated viral DNA after 2D agarose gel electrophoresis. Following Southern blotting, either AbMV DNA was probed with full-length DNA A (a) or methylated DNA was visualized with m5C antibody (b). In an independent experiment, viral DNA (100 ng total nucleic acid from AbMV-infected *N. benthamiana* plants harvested at 21 dpi) was kept untreated (c) or treated with McrBC (d) and then analyzed by 2D agarose gel electrophoresis (first dimension, 0.3% SDS; second dimension, 20 μg/ml chloroquine; 19 h at 45 V). Southern blots were hybridized (c and d) with a probe based on AbMV DNA A lacking the intergenic region. The most prominent viral DNA forms are as described in the legend to Fig. 5 and also included heterogeneous linear dsDNA (h and h′), recombination-dependent replication intermediates (RDR), complementary strand replication intermediates (CSR), and dimeric forms (2×).

ssDNA with a high resolution (Fig. 6a), by hybridization and, in parallel, by use of antibodies directed against methylated bases (Fig. 6b). Among five blots, the blot with the maximal signal for the detection of m5C with antibodies is shown; the others varied by having a spot only at position h′ (Fig. 6b) or intermediates with growing arcs of hdsDNA. No signal was detectable at the positions of viral circular DNA forms in any case. The m5C arc (Fig. 6b) may result from sheared host DNA as well as from viral hdsDNA, which cannot be discriminated with this technique. It is difficult to estimate the detection level under these conditions, and it therefore remains possible that some circular viral molecules have escaped detection.

Therefore, McrBC digestion was applied as described above, and the products were separated in 2D gels. As for the 1D gels (Fig. 5), the most prominent effects of the digestion were the

reduction of heterogeneous linear dsDNA (Fig. 6c and d, spots h) and the increase of the linear dsDNA level (Fig. 6c and d, spots lin).

In summary, the results of all experiments suggest that only a minor portion of geminivirus DNA is methylated and that heterogeneous linear dsDNA is the main target of this modification. The concentration of methylated cytosines in the DNA population of the investigated geminiviruses in the chosen host and under the respective environmental conditions remained low even after prolonged infection periods. It was surely far below the reported 50% level revealed by bisulfite sequencing.

DISCUSSION

The results described here indicate a lower quantitative contribution of methylated nucleotides during the chosen geminivirus infection without rejecting the hypothesis that concomitant transcriptional gene silencing is a host defense mechanism. DNA methylation may influence the race between virus and host in a stochastic and dynamic way, as extensively reviewed in great detail (61). However, our findings stress the importance of proper controls for bisulfite sequencing-based conclusions before assigning an unconverted C as potentially methylated, as critically described before (78). Unfortunately, we cannot compare our data with those in the literature because results showing the reproducibility of the control experiments have not been reported in other publications (11, 60, 62).

The ability of the Phi29 polymerase to amplify bisulfite-converted DNA is demonstrated here for the first time. Bisulfite-treated DNA is a challenging template for DNA polymerases because the presence of uracil needs to be tolerated (78). In our study, the amount of RCA products obtained with bisulfite-treated DNA was optimized by lowering the incubation temperature to 4°C and thereby reducing the polymerization speed. Using random hexamer primers, we expected to obtain the complete pool of bisulfite-converted circular DNA genomes, concomitantly excluding linear DNAs and circumventing the complicated design of nonselective primers.

Usually, 84 to 96% of treated DNA is degraded during conventional bisulfite reactions, resulting in a high loss of template (26). The commercial kit (EpiTect; Qiagen, Hilden, Germany) used in the current study has been reported to generate conversion levels of over 99%, with only modest DNA degradation (58). However, with increasing lengths of target sequence, template loss due to single-strand breaks will enhance selection for unmodified C's. This is particularly the case for RCA, since a single break in the circular template completely abolishes the reaction. Therefore, a proper control template to ensure complete conversion of unmethylated C's should be similar in length and conformation to the DNA molecules being analyzed and treated in the same manner. The single-stranded bacteriophage DNA used in this study fulfilled most of these requirements and provoked a more cautious evaluation of the data set. DNAs of filamentous phages have been used before as essentially nonmethylated templates (26). Low percentages of methylation of either adenine or cytosine have been reported for single-stranded DNA-containing phages (21, 32, 33, 77).

Published reports have shown probabilities of 50% cytosine methylation for the intergenic region of cabbage leaf curl begomovirus DNA A and for the beet curly top curtovirus (BCTV), as determined by bisulfite conversion followed by PCR (60), or probabilities of 36% for symmetric and 46% for asymmetric sites for tomato leaf curl begomovirus ORF C1 (4). Cytosine methylation of the viral genome was found to be stimulated in plants transgenic for the analyzed sequences, leading to 55% protected symmetric and 47.5% protected asymmetric sites (4). Extreme methylation rates of up to 80% have been reported for BCTV constructs with mutated silencing suppressors in recovered *Arabidopsis thaliana* wt tissues (60). In contrast, analyses of pepper golden mosaic virus indicated no more than about 10% methylated cytosines in the intergenic region and 2% methylated cytosines in the coat protein region at 10 dpi, followed by increases to 25% in the intergenic region and to 10% in the coat protein region after recovery of the plants at 15 dpi, with similar proportions between symmetrical and asymmetrical sites in older and younger leaves (62). These results indicate significant variability between different virus-host combinations analyzed, with reference to the virus and host and, in particular, to recovery phenomena. AbMV induces mild symptoms in *N. benthamiana* plants during the observed period of infection and may thus trigger a lower defense response by the plant. It would be extremely interesting to determine how nonmethylated control DNAs behave in the environment of the specific combinations of plant tissues and viruses used in the assay. Changing viral DNA concentrations in the particular sample should influence the result, as discussed for repetitive DNA depending on the C_0t (78).

Here we analyzed complete geminivirus genome components for the first time and were therefore able to judge the overall variation. Only in a short stretch of the TYLCSV DNA sequence did the number of protected C's exceed the threshold value. This stretch is located within ORF C1, in a highly conserved region which was found to bind plant transcription factors promoting the transcription of a 0.7-kb complementary-sense mRNA of tomato golden mosaic virus (70). Methylation of the respective DNA region may therefore function in transcriptional control. Further studies on this locus in different geminiviruses are needed, however, before final conclusions can be drawn. For the rest of the sites that exceeded the threshold value, the statistical basis of the data is too low so far to judge the significance of the results.

All of our sequencing data are consistent with the experimental results yielded by immunological detection of m5C (Fig. 6) and with the restriction enzyme-based analysis (Fig. 1). Monoclonal antibodies directed against m5C (57) have confirmed induced demethylation in *Arabidopsis* (64). Here we combined blot immunolabeling with 2D gel electrophoresis (40), for the first time, in order to differentiate between linear and circular DNAs in the analysis. Methylated plant genomic DNA was detected most efficiently, showing the feasibility of this approach. However, linear viral DNA could not be differentiated from the comigrating excess of plant nucleic acid. If the circular virus DNA had been a target of methylation at all, its amount was below the detection limit of the technique. The data resulting from RFLP analyses of the source DNA before (Fig. 1) and after (Fig. 2 and 3) RCA did not support a high level of methylation either. Fragments with molecular weights

deviating from expectations do not really prove methylation, because the sensitive detection technique used here also allowed us to monitor mutational polymorphisms in the quasispecies population of viral DNA molecules, and ssDNA molecules with incomplete second-strand synthesis can lead to the same result (see reference 39 for further discussion).

The application of methylation-dependent restriction enzymes allowed a more direct determination of methylated bases, and the results support the conclusions of the aforementioned experiments. This approach reveals, for the first time in the virology of geminiviruses, a more quantitative estimation of the relevance of methylation and a discrimination between differently affected DNA conformations when the approach is used in combination with chloroquine-aided 1D and 2D electrophoresis. On this basis, it became clear that the heterogeneous linear dsDNA was the main target of methylation, whereas ocDNA, ssDNA, and cccDNA were not or were considerably less modified.

In summary, our results demonstrate that the major proportion of the investigated geminivirus DNA is not methylated. Nevertheless, they do not exclude a role of methylation during viral infection. Methylation may participate in plant defense to suppress viral multiplication. It might be induced by overlapping viral mRNAs from sense and complementary-sense transcription and subsequent RNA-directed DNA methylation. In a productive infection, however, methylated viral DNA will be overgrown by the unmethylated viral progeny that has escaped plant defense. Obviously, the replication modes of geminiviruses are highly efficient because of the use of RCR and RDR, which resurrect DNA molecules from methylation.

ACKNOWLEDGMENTS

This work was supported by DFG grant Je 116/10-3, by a trilateral ERA-PG/BMBF project (to H.J.) (BMBF 0313986), and by COST grant FA0806.

We thank M. Wassenegger for asking the right questions, R. Burdick and C. Wege for critically reading the manuscript, and the gardeners D. Gotthardt and A. Allinger for taking care of the plants.

REFERENCES

1. **Abouzid, A. M., T. Frischmuth, and H. Jeske.** 1988. A putative replicative form of the abutilon mosaic virus (gemini group) in a chromatin-like structure. Mol. Gen. Genet. **212:**252–258.
2. **Akbergenov, R., et al.** 2006. Molecular characterization of geminivirus-derived small RNAs in different plant species. Nucleic Acids Res. **34:**462–471.
3. **Alberter, B., A. M. Rezaian, and H. Jeske.** 2005. Replicative intermediates of ToLCV and its satellite DNAs. Virology **331:**441–448.
4. **Bian, X.-Y., M. S. Rasheed, M. Seemanpillai, and A. Rezaian.** 2006. Analysis of silencing escape of tomato leaf curl virus: an evaluation of the role of DNA methylation. Mol. Plant Microbe Interact. **19:**614–624.
5. **Bird, A.** 2002. DNA methylation patterns and epigenetic memory. Genes Dev. **16:**6–21.
6. **Bisaro, D. M.** 2006. Silencing suppression by geminivirus proteins. Virology **344:**158–168.
7. **Blevins, T., et al.** 2006. Four plant Dicers mediate viral small RNA biogenesis and DNA virus induced silencing. Nucleic Acids Res. **34:**6233–6246.
8. **Böttcher, B., S. Unseld, H. Ceulemans, R. B. Russell, and H. Jeske.** 2004. Geminate structures of African cassava mosaic virus. J. Virol. **78:**6758–6765.
9. **Brandes, J. C., H. Carraway, and J. G. Herman.** 2007. Optimal primer design using the novel primer design program: MSPprimer provides accurate methylation analysis of the ATM promoter. Oncogene **26:**6229–6237.
10. **Brough, C. L., et al.** 1992. DNA methylation inhibits propagation of tomato golden mosaic virus DNA in transfected protoplasts. Plant Mol. Biol. **18:** 703–712.
11. **Buchmann, R. C., S. Asad, J. N. Wolf, G. Mohannath, and D. M. Bisaro.** 2009. Geminivirus AL2 and L2 proteins suppress transcriptional gene silencing and cause genome-wide reductions in cytosine methylation. J. Virol. **83:**5005–5013.
12. **Cai, X., et al.** 2007. Efficient gene silencing induction in tomato by a viral satellite DNA vector. Virus Res. **125:**169–175.
13. **Carrillo-Tripp, J., H. Shimada-Beltran, and R. Rivera-Bustamante.** 2006. Use of geminiviral vectors for functional genomics. Curr. Opin. Plant Biol. **9:**209–215.
14. **Clark, S. J., J. Harrison, C. L. Paul, and M. Frommer.** 1994. High sensitivity mapping of methylated cytosines. Nucleic Acids Res. **22:**2990–2997.
15. **Cohen-Karni, D., et al.** 2011. The MspJI family of modification-dependent restriction endonucleases for epigenetic studies. Proc. Natl. Acad. Sci. U. S. A. **108:**11040–11045.
16. **Csorba, T., V. Pantaleo, and J. Burgyan.** 2009. RNA silencing: an antiviral mechanism. Adv. Virus Res. **75:**35–71.
17. **Erdmann, J. B., et al.** 2010. Replicative intermediates of maize streak virus found during leaf development. J. Gen. Virol. **91:**1077–1081.
18. **Ermak, G., U. Paszkowski, M. Wohlmuth, O. Mittelsten Scheid, and J. Paszkowski.** 1993. Cytosine methylation inhibits replication of African cassava mosaic virus by two distinct mechanisms. Nucleic Acids Res. **25:**3445–3450.
19. **Fedoreyeva, L. I., and B. F. Vanyushin.** 2002. N6-adenine DNA-methyltransferase in wheat seedlings. FEBS Lett. **514:**305–308.
20. **Fofana, I. B., A. Sangare, R. Collier, C. Taylor, and C. M. Fauquet.** 2004. A geminivirus-induced gene silencing system for gene function validation in cassava. Plant Mol. Biol. **56:**613–624.
21. **Friedman, J., A. Friedmann, and A. Razin.** 1977. Studies on the biological role of DNA methylation. III. Role in excision of one-genome long single-stranded phi X174 DNA. Nucleic Acids Res. **4:**3483–3496.
22. **Frischmuth, T., G. Zimmat, and H. Jeske.** 1990. The nucleotide sequence of abutilon mosaic virus reveals prokaryotic as well as eukaryotic features. Virology **178:**461–468.
23. **Frommer, M., et al.** 1992. A genomic sequencing protocol that yields a positive display of 5-methylcytosine residues in individual DNA strands. Proc. Natl. Acad. Sci. U. S. A. **89:**1827–1831.
24. **Fulnecek, J., R. Matyasek, A. Kovarik, and M. Bezdek.** 1998. Mapping of 5-methylcytosine residues in Nicotiana tabacum 5S rRNA genes by genomic sequencing. Mol. Gen. Genet. **259:**133–141.
25. **Goll, M. G., and T. H. Bestor.** 2005. Eukaryotic cytosine methyltransferases. Annu. Rev. Biochem. **74:**481–514.
26. **Grunau, C., S. J. Clark, and A. Rosenthal.** 2001. Bisulfite genomic sequencing: systematic investigation of critical experimental parameters. Nucleic Acids Res. **29:**E65–5.
27. **Gruntman, E., et al.** 2008. Kismeth: analyzer of plant methylation states through bisulfite sequencing. BMC Bioinformatics **9:**371.
28. **Hagen, C., M. R. Rojas, T. Kon, and R. L. Gilbertson.** 2008. Recovery from cucurbit leaf crumple virus (family Geminiviridae, genus Begomovirus) infection is an adaptive antiviral response associated with changes in viral small RNAs. Phytopathology **98:**1029–1037.
29. **Haible, D., S. Kober, and H. Jeske.** 2006. Rolling circle amplification revolutionizes diagnosis and genomics of geminiviruses. J. Virol. Methods **135:** 9–16.
30. **Hall, T. A.** 1999. BioEdit: a user-friendly biological sequence alignment editor and analysis program for Windows 95/98/NT. Nucleic Acids Symp. Ser. **41:**95–98.
31. **Hanley-Bowdoin, L., S. B. Settlage, B. M. Orozco, S. Nagar, and D. Robertson.** 1999. Geminiviruses: models for plant DNA replication, transcription, and cell cycle regulation. Crit. Rev. Plant Sci. **18:**71–106.
32. **Hattmann, S.** 1973. Plasmid-controlled variation in the content of methylated bases in single-stranded DNA bacteriophages M13 and fd. J. Mol. Biol. **74:**749–752.
33. **Hattmann, S., C. Gribbin, and C. A. Hutchinson.** 1979. In vivo methylation of bacteriophage phi X174 DNA. J. Virol. **32:**845–851.
34. **Hehnle, S., C. Wege, and H. Jeske.** 2004. The interaction of DNA with the movement proteins of geminiviruses revisited. J. Virol. **78:**7698–7706.
35. **Hetzl, J., A. M. Foerster, G. Raidl, and O. Mittelsten Scheid.** 2007. CyMATE: a new tool for methylation analysis of plant genomic DNA after bisulphite sequencing. Plant J. **51:**526–536.
36. **Homs, M., S. Kober, G. Kepp, and H. Jeske.** 2008. Mitochondrial plasmids of sugar beet amplified via rolling circle method detected during curtovirus screening. Virus Res. **136:**124–129.
37. **Jeske, H.** 2009. Geminiviruses. Curr. Top. Microbiol. Immunol. **331:**185–226.
38. **Jeske, H.** 2007. Replication of geminiviruses and the use of rolling circle amplification for their diagnosis, p. 141–156. *In* H. Czosnek (ed.), Tomato yellow leaf curl virus disease. Springer, Dordrecht, Netherlands.
39. **Jeske, H., D. Gotthardt, and S. Kober.** 2010. In planta cloning of geminiviral DNA: the true Sida micrantha mosaic virus. J. Virol. Methods **163:**301–308.
40. **Jeske, H., M. Lütgemeier, and W. Preiss.** 2001. Distinct DNA forms indicate rolling circle and recombination-dependent replication of abutilon mosaic geminivirus. EMBO J. **20:**6158–6167.
41. **Jovel, J., W. Preiss, and H. Jeske.** 2007. Characterization of DNA-intermediates of an arising geminivirus. Virus Res. **130:**63–70.
42. **Kittelmann, K., and H. Jeske.** 2008. Disassembly of African cassava mosaic virus. J. Gen. Virol. **89:**2029–2036.

43. **Kjemtrup, S., et al.** 1998. Gene silencing from plant DNA carried by a geminivirus. Plant J. **14:**91–100.
44. **Korch, C., and P. Hagblom.** 1986. In-vivo-modified gonococcal plasmid pJD1. A model system for analysis of restriction enzyme sensitivity to DNA modifications. Eur. J. Biochem. **161:**519–524.
45. **Krenz, B., C. Wege, and H. Jeske.** 2010. Cell-free construction of disarmed abutilon mosaic virus-based gene silencing vectors. J. Virol. Methods **169:** 129–137.
46. **Li, L. C.** 2007. Designing PCR primer for DNA methylation mapping. Methods Mol. Biol. **402:**371–384.
47. **Li, L. C., and R. Dahiya.** 2002. MethPrimer: designing primers for methylation PCRs. Bioinformatics **18:**1427–1431.
48. **Marshall, O.** 2007. Graphical design of primers with PerlPrimer. Methods Mol. Biol. **402:**403–414.
49. **Moffat, A.** 1999. Geminiviruses emerge as serious crop threat. Science **286:** 1835.
50. **Morilla, G., B. Krenz, H. Jeske, E. R. Bejarano, and C. Wege.** 2004. Tête à tête of tomato yellow leaf curl virus (TYLCV) and tomato yellow leaf curl Sardinia virus (TYLCSV) in single nuclei. J. Virol. **78:**10715–10723.
51. **Muangsan, N., and D. Robertson.** 2004. Geminivirus vectors for transient gene silencing in plants. Methods Mol. Biol. **265:**101–115.
52. **Paprotka, T., et al.** 2010. Genomic diversity of sweet potato geminiviruses in a Brazilian germplasm bank. Virus Res. **149:**224–233.
53. **Paprotka, T., V. Metzler, and H. Jeske.** 2010. The complete nucleotide sequence of a new bipartite abutilon infecting begomovirus species from Brazil. Arch. Virol. **155:**813–816.
54. **Paprotka, T., V. Metzler, and H. Jeske.** 2010. The first DNA 1-like alpha satellites in association with New World begomoviruses in natural infections. Virology **404:**148–157.
55. **Pilartz, M., and H. Jeske.** 1992. Abutilon mosaic geminivirus double-stranded DNA is packed into minichromosomes. Virology **189:**800–802.
56. **Pilartz, M., and H. Jeske.** 2003. Mapping of abutilon mosaic geminivirus minichromosomes. J. Virol. **77:**10808–10818.
57. **Podesta, A., M. R. Castiglione, S. Avanzi, and G. Montagnoli.** 1993. Molecular geometry of antigen binding by a monoclonal antibody against 5-methylcytidine. Int. J. Biochem. **25:**929–933.
58. **Pomraning, K. R., K. M. Smith, and M. Freitag.** 2009. Genome-wide high throughput analysis of DNA methylation in eukaryotes. Methods **47:**142–150.
59. **Preiss, W., and H. Jeske.** 2003. Multitasking in replication is common among geminiviruses. J. Virol. **77:**2972–2980.
60. **Raja, P., B. C. Sanville, R. C. Buchmann, and D. M. Bisaro.** 2008. Viral genome methylation as an epigenetic defense against geminiviruses. J. Virol. **82:**8997–9007.
61. **Raja, P., J. N. Wolf, and D. M. Bisaro.** 2010. RNA silencing directed against geminiviruses: post-transcriptional and epigenetic components. Biochim. Biophys. Acta **1799:**337–351.
62. **Rodriguez-Negrete, E. A., J. Carrillo-Tripp, and R. F. Rivera-Bustamante.** 2009. RNA silencing against geminivirus: complementary action of posttranscriptional gene silencing and transcriptional gene silencing in host recovery. J. Virol. **83:**1332–1340.
63. **Sambrook, J., and D. W. Russell.** 2001. Molecular cloning: a laboratory manual, 3rd ed. Cold Spring Harbor Laboratory Press, Cold Spring Harbor, NY.
64. **Scebba, F., et al.** 2003. Arabidopsis MBD proteins show different binding specificities and nuclear localization. Plant Mol. Biol. **53:**715–731.
65. **Seemanpillai, M., I. Dry, J. Randles, and A. Rezaian.** 2003. Transcriptional silencing of geminiviral promoter-driven transgenes following homologous virus infection. Mol. Plant Microbe Interact. **16:**429–438.
66. **Srivastava, G. P., J. Guo, H. Shi, and D. Xu.** 2008. PRIMEGENS-v2: genome-wide primer design for analyzing DNA methylation patterns of CpG islands. Bioinformatics **24:**1837–1842.
67. **Stanley, J., et al.** 2005. Geminiviridae, p. 301–326. *In* C. M. Fauquet, M. A. Mayo, J. Maniloff, U. Desselberger, and L. A. Ball (ed.), Virus taxonomy. VIIIth report of the International Committee on Taxonomy of Viruses. Elsevier/Academic Press, London, United Kingdom.
68. **Sulewska, A., et al.** 2007. Detection of DNA methylation in eucaryotic cells. Folia Histochem. Cytobiol. **45:**315–324.
69. **Tanious, F. A., J. M. Veal, H. Buczak, L. S. Ratmeyer, and W. D. Wilson.** 1992. DAPI (4′,6-diamidino-2-phenylindole) binds differently to DNA and RNA: minor-groove binding at AT sites and intercalation at AU sites. Biochemistry **31:**3103–3112.
70. **Tu, J., and G. Sunter.** 2007. A conserved binding site within the tomato golden mosaic virus AL-1629 promoter is necessary for expression of viral genes important for pathogenesis. Virology **367:**117–125.
71. **Tusnady, G. E., I. Simon, A. Varadi, and T. Aranyi.** 2005. BiSearch: primer-design and search tool for PCR on bisulfite-treated genomes. Nucleic Acids Res. **33:**e9.
72. **Vanderschuren, H., M. Stupak, J. Futterer, W. Gruissem, and P. Zhang.** 2007. Engineering resistance to geminiviruses—review and perspectives. Plant Biotechnol. J. **5:**207–220.
73. **Vanitharani, R., P. Chellappan, and C. M. Fauquet.** 2005. Geminiviruses and RNA silencing. Trends Plant Sci. **10:**144–151.
74. **Vanyushin, B. F.** 2005. Enzymatic DNA methylation is an epigenetic control for genetic functions of the cell. Biochemistry (Moscow) **70:**488–499.
75. **Voinnet, O.** 2005. Induction and suppression of RNA silencing: insights from viral infections. Nat. Rev. Genet. **6:**206–220.
76. **Wang, M. B., and M. Metzlaff.** 2005. RNA silencing and antiviral defense in plants. Curr. Opin. Plant Biol. **8:**216–222.
77. **Wang, R. Y.-H., S. Shenoy, and M. Ehrlich.** 1984. DNA methylation inhibits the transfecting activity of replicative-form phi X174 DNA. J. Virol. **49:**674–679.
78. **Warnecke, P. M., et al.** 2002. Identification and resolution of artifacts in bisulfite sequencing. Methods **27:**101–107.
79. **Wege, C.** 2007. Movement and localization of tomato yellow leaf curl viruses in the infected plant, p. 185–206. *In* H. Czosnek (ed.), Tomato yellow leaf curl virus disease. Springer, Dordrecht, Netherlands.
80. **Wege, C., R. D. Gotthardt, T. Frischmuth, and H. Jeske.** 2000. Fulfilling Koch's postulates for abutilon mosaic virus. Arch. Virol. **145:**2217–2225.
81. **Wege, C., and D. Siegmund.** 2007. Synergism of a DNA and an RNA virus: enhanced tissue infiltration of the begomovirus abutilon mosaic virus (AbMV) mediated by cucumber mosaic virus (CMV). Virology **357:**10–28.
82. **Wyant, P. S., D. Gotthardt, B. Schäfer, B. Krenz, and H. Jeske.** 2011. The genomes of four novel begomovirus species and a new Sida micrantha mosaic virus strain from Bolivian weeds. Arch. Virol. **156:**347–352.
83. **Zhang, W., et al.** 2001. Structure of the maize streak virus geminate particle. Virology **279:**471–477.
84. **Zhu, J. K.** 2009. Active DNA demethylation mediated by DNA glycosylases. Annu. Rev. Genet. **43:**143–166.
85. **Zilberman, D., M. Gehring, R. K. Tran, T. Ballinger, and S. Henikoff.** 2007. Genome-wide analysis of Arabidopsis thaliana DNA methylation uncovers an interdependence between methylation and transcription. Nat. Genet. **39:**61–69.
86. **Zilberman, D., and S. Henikoff.** 2007. Genome-wide analysis of DNA methylation patterns. Development **134:**3959–3965.